

# Cosmological aspects of a hyperbolic solution in $f(R, T)$ theory of gravity

Lokesh Kumar Sharma<sup>a</sup>, Suresh Parekh<sup>c,\*</sup>, Vaibhav Trivedi<sup>d,\*</sup>, Saibal Ray<sup>e</sup>, Anil Kumar Yadav<sup>1</sup>

<sup>a</sup>Department of Physics, GLA University, Mathura 281406, Uttar Pradesh, India

<sup>b</sup>Department of Physics, SP Pune University, Pune 411007, Maharashtra, India

<sup>c</sup>Department of Physics, Fergusson College, Pune 411007, Maharashtra, India

<sup>d</sup>Centre for Cosmology, Astrophysics and Space Science (CCASS), GLA University, Mathura 281406, Uttar Pradesh, India

<sup>e</sup>Department of Physics, United College of Engineering and Research, Greater Noida 201 306, India

---

## Abstract

This paper is about the cosmological framework of  $f(R, T)$  gravity for a flat Friedmann-Lemaître-Robertson-Walker (FLRW) model of the universe. It is an approach that combines the  $f(R, T)$  function with a mixture of  $f(R)$  and  $f(T)$ , where the former involves quadratic geometric corrections ( $f(R) = R + \alpha R^2$ ) and the latter represents linear matter term ( $f(T) = 2\lambda T$ ). By introducing a geometrical parameter using the scale factor  $a(t) = \sinh^{\frac{1}{n}}(\beta t)$  [1], where  $\beta$  and  $n$  are model parameters, we solve gravitational field equations in terms of the  $f(R, T)$ . The model predicts eternal acceleration for  $0 < n < 1$  while transitioning to its present accelerated phase following an early decelerated era for  $n \geq 1$ . The model's implications include cosmic structure formation driven by a transition from a dominated era to a dominated era governed by Jean's instability condition. The inquiry into  $\omega$  as varying EoS parameters and examining scalar field behavior apart from discussing energy conditions on an obtained solution. The model's validity is assessed through comprehensive analysis using jerk, lerk, snap parameters, state finder diagnostic, and om diagnostic. Additionally, the study exploits several observations, including  $H(z)$  BAO data, SNeIa, and their joint combinations to constrain  $\beta$ ,  $n$  and  $q$ . The results indicate that the model agrees with these observations, consistent with the current understanding of cosmology.

---

**Keywords:** Cosmological Parameters, Hyperbolic scale factor, Observational constraints, Om Diagnostics, Cosmography, MCMC Model

## 1. Introduction

The Einstein Field Equations are as follows in equation (1) where  $g_{ij}$  is the second order covariant metric tensor,  $R_j^i$  is the Ricci tensor,  $R$  is the Ricci scalar,  $T_{ij}$  is the third rank energy-momentum tensor,  $\Lambda$  is the cosmological constant, and  $G$ , and  $c$ . There are also potential alternatives for general relativity, which are motivated by many other things, such as its enigmatic

---

\*Saibal Ray

Email addresses: lokesh.sharma@gla.ac.in (Lokesh Kumar Sharma), thesureshparekh@gmail.com (Suresh Parekh), vbtrivedi06@gmail.com (Vaibhav Trivedi), saibal.ray@gla.ac.in (Saibal Ray), abanilyadav@yahoo.co.in (Anil Kumar Yadav)

nature of matter content that makes about 95% of the universe's contents unknown. Although general relativity has been experimentally verified to be correct, it is faced with some challenges in reconciling with quantum mechanics. For instance, there is a singularity at the initial moment of Big Bang spacetime whose quantization remains unresolved. Quantum Mechanics and GR form two bases for modern physics that must be unified. Even though the  $\Lambda$ CDM model has had a fantastic success, some issues cannot be resolved, like the fine-tuning problem, which should have prompted a search for alternative theories of gravity.

$$R_{ij} + \frac{1}{2}Rg_{ij} + \Lambda g_{ij} = \frac{8\pi G}{c^4}T_{ij} \quad (1)$$

The modified gravity theories include  $f(R)$  gravity, a better alternative than others as it considers Ricci scalar's general function in the Einstein-Hilbert action. The different surveys carried out on the  $f(R)$  gravity have indicated that despite the absence of a cosmological constant, it can be used to show both cosmic acceleration phases. However, this theory fails these tests, such as observations of galaxies' rotation curves and dynamics of planets. This formulation can effectively deal with these issues by incorporating  $f(R, T)$  gravity, where the matter Lagrangian is given as a function of EMT trace. As such, there are good proposals for observational difficulties, including exotic imperfect fluids and quantum effects. The developing field of  $f(R, T)$  gravity has made substantial contributions to cosmology and astrophysics, including its capability to solve the dark matter problem.

The above investigation has inspired the formulation of a cosmological framework within the context of  $f(R, T)$  gravity along with observational analysis parameter estimation using the  $H(z)$ , BAO, and Pantheon Datasets. The structure of the paper goes as follows. In Section 2, we discuss the  $f(R, T)$  theory and derive highly non-linear field equations by splitting the  $f(R, T)$  function into a quadratic  $R$ -dependent term and a linear  $T$ -dependent term. In Section 3, we discuss the observational analysis and obtained parameter values. Also, we demonstrate the Energy Conditions, Jerk parameter, lerk Parameter, snap parameter, and State Finder Diagnostics. And to summarize our findings and outcomes of our tests, we provide a brief conclusion in form of Section 4.

## 2. Mathematical background of $f(R, T)$ cosmology

The comprehensive action corresponding to  $f(R, T) = f(R) + 2f(T)$  gravity, as presented in [2], is associated with the action of a matter field described by the matter Lagrangian  $S_m$ :

$$S = \int \left( \frac{1}{16\pi G} f(R, T) + S_m \right) \sqrt{-g} dx^4 \quad (2)$$

In the context of our investigation, the function  $f(R, T)$  is regarded as an arbitrary function of the Ricci scalar  $R$  and the trace of the energy-momentum tensor  $T$ . Specifically, we adopt the expression  $f(R) = R + \alpha R^2$ , initially proposed by Starobinsky, as our foundational model for inflationary dynamics [3]. This formulation of  $f(R)$  finds its roots in the quantum corrections to the Friedmann equations. Including the  $R^2$  term in the functional form of  $f(R)$  is a natural correction to General Relativity (GR), inherently offering an inflationary framework for the early Universe. Furthermore, the Starobinsky model exhibits remarkable consistency with the latest cosmological observations [4], emerging as a compelling alternative to scalar field models characterizing inflation [5].

Expanding upon the previous  $f(R)$  form by incorporating negative exponents of the curvature term enables the representation of recent cosmic acceleration. Thus, within the framework of the general model  $f(R) = R + \alpha R^m + \beta R^{1/n}$ , where  $\alpha$  and  $\beta$  represent arbitrary constants, both early and late-time cosmic acceleration phenomena find explanation through theories extending beyond GR [6].

In order to introduce exotic imperfect fluids and incorporate quantum effects into the aforementioned  $f(R)$  model, a term dependent on the trace  $T$  is imperative. This source term, contingent on the matter Lagrangian  $S_m$ , yields a well-defined set of field equations. Our study considers  $f(T)$  a linear function of  $T$ , defined explicitly as  $f(T) = 2\lambda T$ . Thus, the complete form of the  $f(R, T)$  function assumes the expression  $R + \alpha R^2 + 2\lambda T$ .

On defining EMT of matter [2]

$$T_{ij} = \frac{2}{\sqrt{-q}} \frac{\delta(\sqrt{-g}S_m)}{\delta g^{ij}}, \quad (3)$$

where, the trace is defined as  $T = g^{ij}T_{ij}$ . Moreover, should  $S_m$  solely depend on  $g^{ij}$ , it allows for the expression

$$T_{ij} = g_{ij}S_m - 2\frac{\delta S_m}{\delta g^{ij}}, \quad (4)$$

Taking variation of action (3) w.r.t.  $g_{ij}$  we have

$$f^R(R, T)R_{ij} - \frac{1}{2}g_{ij}f(R, T) + (g_{ij}\square - \nabla_i\nabla_j)f^R(R, T) = 8\pi GT_{ij} - f^T(R, T)(T_{ij} + \Theta_{ij}) \quad (5)$$

where,  $f_R(R, T)$  and  $f_T(R, T)$  denote the derivatives of  $f(R, T)$  with respect to  $R$  and  $T$  respectively. The d'Alembert operator  $\square$  is defined as  $\square = g^{ij}\nabla_i\nabla_j$ , where  $\nabla_i$  represents the covariant derivative with respect to  $g_{ij}$  associated with the symmetric Levi-Civita connection. The expression  $\Theta_{ij}$  is structured as follows:

$$\Theta_{ij} \equiv g^{lm}\frac{\delta T_{lm}}{\delta g_{ij}} = -2T_{ij} + g_{ij}S_m - 2g^{lm}\frac{\delta^2 S_m}{\delta g_{ij}\delta g^{lm}} \quad (6)$$

In the present study, we examine a perfect fluid system in a state of thermodynamic equilibrium. Thus, we adopt the straightforward approach of setting the matter Lagrangian  $S_m$  to be equal to minus the pressure  $p$  while considering the Energy-Momentum Tensor (EMT) of matter as follows:

$$T_{ij} = (\rho + p)u_i u_j - pg_{ij} \quad (7)$$

where  $\rho$  is the energy density, and  $p$  is the pressure of the fluid present in the Universe. Employing equation (6), we derive the variation expression for the Energy-Momentum Tensor (EMT) of a perfect fluid as follows:

$$\Theta_{ij} = -2T_{ij} - pg_{ij} \quad (8)$$

Substituting Equation (8) in Equation (5), the gravitational equation of motion is formulated as:

$$f^R(R, T)R_{ij} - \frac{1}{2}g_{ij}f(R, T) + (g_{ij}\square - \nabla_i\nabla_j)f^R(R, T) = 8\pi GT_{ij} + f^T(R, T)(T_{ij} + pg_{ij}). \quad (9)$$

We observe the relationship between the Ricci Scalar  $R$  and  $T$  by contracting Equation (9) with respect to  $g_{ij}$  as:

$$Rf^R(R, T) - 2f(R, T) + 3\Box f^R(R, T) = 8\pi GT + (T + 4p)f^T(R, T) \quad (10)$$

By rearranging the terms in Equation (8), the Ricci tensor  $R_{ij}$  adopts the form

$$R_{ij} = \frac{1}{f^R(R, T)} \left( 8\pi GT_{ij} + \frac{1}{2}g_{ij} + (\nabla_i \nabla_j - g_{ij}\Box)f^R(R, T) + f^T(R, T)(T_{ij} + pg_{ij}) \right) \quad (11)$$

$\Diamond_{ij}$  is defined as,

$$\Diamond_{ij} = \nabla_i \nabla_j - g_{ij}\Box \quad (12)$$

We can rewrite Equation (11) as

$$R_{ij} = \frac{1}{f^R(R, T)} \left( 8\pi GT_{ij} + \frac{1}{2}g_{ij} + \Diamond_{ij}f^R(R, T) + f^T(R, T)(T_{ij} + pg_{ij}) \right) \quad (13)$$

Thus, we obtain the expression of Ricci Scalar  $R$  by re-arranging the terms in Equation (10) as

$$R = \frac{1}{f^R(R, T)} (8\pi GT + 2f(R, T) - 3\Box f^R(R, T) + (T + 4p)f^T(R, T)) \quad (14)$$

Using the above obtained Equations (13) and (14), Equation (9) can be represented in terms of Einstein tensor  $G_{ij}$ ,

$$\begin{aligned} G_{ij} &= R_{ij} - \frac{1}{2}Rg_{ij} - \frac{8\pi GT_{ij}}{f^R(R, T)} + \frac{1}{f^R(R, T)} \left[ \frac{1}{2}g_{ij}(f(R, T) - Rf^R(R, T)) \right. \\ &\quad \left. + \Diamond_{ij}f^R(R, T) + T_{ij} + pg_{ij}f^T(R, T) \right] \\ &= \frac{8\pi G}{f^R(R, T)} (T_{ij} + T'_{ij}) \end{aligned} \quad (15)$$

where  $T'_{ij} = \frac{1}{8\pi G} \left( \frac{1}{2}g_{ij}(f(R, T)) + \Diamond_{ij}f^R(R, T) + (T_{ij} + pg_{ij}f^T(R, T)) \right)$

The preceding set of equations highlights that the Einstein Field Equations (EFE) in General Relativity (GR) can be simplified by setting  $\alpha = 0$  and  $\lambda = 0$ . Upon applying the Bianchi identity to Equation (15), we arrive at <sup>1</sup>

$$(8\pi G + f^T(R, T)) \nabla^i T_{ij} + \frac{1}{2}f^T(R, T)\nabla_i T + T_{ij}\nabla^i f^T(R, T) + \nabla_j (pf^T(R, T)) = 0 \quad (16)$$

We explore the dynamics of the Universe through an examination of a spatially flat FLRW line element characterized by its homogeneity and isotropy as

$$ds^2 = dt^2 - a^2(t)(dx^2 + dy^2 + dz^2) \quad (17)$$

---

<sup>1</sup>Please be aware that the equation referenced in [??] has been derived previously. However, due to the differing metric signature utilized in the current study, the final term in Equation (16) has acquired an opposite sign.

where  $a(t)$  is the scale factor. The trace  $T$  in EMT Equation (7) and scale curvature  $R$  are

$$T = \rho - 3p \quad (18)$$

$$R = -6(2H^2 + \dot{H}) \quad (19)$$

where  $H$  is the bubble parameter defined as  $\frac{\dot{a}}{a}$  and the derivative on  $a$  suggests the differentiation w.r.t.  $t$ . Assuming  $f(R, T) = R + \alpha R^2 + 2\lambda T$  and substituting Equation (7), (18), (19) in Equation (15), we obtain the following field equations

$$3H^2 = \frac{1}{1 + 2\alpha R} [8\pi\rho + \lambda(3\rho - p) + 2\alpha U(a, \dot{a}, \ddot{a}, \ddot{\ddot{a}})] \quad (20)$$

$$2\dot{H} + 3H^2 = \frac{1}{1 + 2\alpha R} [-8p\rho + \lambda(\rho - 3p) + 2\alpha V(a, \dot{a}, \ddot{a}, \ddot{\ddot{a}})] \quad (21)$$

where  $U(a, \dot{a}, \ddot{a}, \ddot{\ddot{a}}) = \frac{-9}{a^4}(5\dot{a}^4 + a\ddot{a}^2 - 2a^2\dot{a}\ddot{\ddot{a}})$  and  $V(a, \dot{a}, \ddot{a}, \ddot{\ddot{a}}) = \frac{3}{a^4}(\dot{a}^4 - 18a\dot{a}^2\ddot{a} + 4a^2\dot{a}\ddot{\ddot{a}} + a^2(-2\dot{a}\ddot{\ddot{a}} + a\ddot{\ddot{\ddot{a}}}))$  are functions of scale factor  $a$  and their derivatives up to forth order respectively. Also, we have set the units such that  $G = 1$ .

Substituting the above values for  $f(R, T)$  in Equation (16) gives

$$\frac{8\pi + 3\lambda}{8\pi + 2\lambda}\dot{\rho} - \frac{\lambda}{8\pi + 2\lambda}\dot{p} + 3H(\rho + p) = 0 \quad (22)$$

Rewriting Equation (20) as

$$(8\pi + 3\lambda)\rho - \lambda p = \mathcal{U} \quad (23)$$

where  $\mathcal{U}$  is defined as

$$\mathcal{U} \equiv 3H^2 + 18\alpha(\dot{H}^2 - 4H^2\dot{H} - 2H\ddot{H}) \quad (24)$$

Solving Equation (22) and (23) gives the form

$$\rho = \frac{3\mathcal{U} - \lambda(8\pi + 2\lambda)^{-1}H^{-1}\dot{\mathcal{U}}}{3(8\pi + 4\lambda)} \quad (25)$$

$$p = \frac{(8\pi + 3\lambda)\rho - \mathcal{U}}{\lambda} \quad (26)$$

Obtained Equations (25) and (26) demonstrate that in order to derive precise solutions for  $\rho$  and  $p$  and to investigate dark energy models, it is essential to employ a parametrization of either  $a(t)$  or  $H(t)$ . This approach, known as a model-independent method for probing dark energy models, necessitates a deliberate selection of  $a(t)$ . In this study, we focus on a temporary determination of  $a(t)$ , which emerges from a time-dependent deceleration parameter (DP) [32] as

$$a(t) = \sinh^{\frac{1}{n}}(\beta t) \quad (27)$$

where  $\beta$  and  $n > 0$  are arbitrary constants.

The Hubble parameter  $H(t)$  and DP  $q(t)$  can be obtained from Equation (27) as

$$H(t) = \frac{\beta \coth(\beta t)}{n} \quad (28)$$

and

$$q(t) = n[1 - \tanh^2(\beta t)] - 1 \quad (29)$$

In this investigation, our interest lies in exploring the various phases of the Universe, specifically the transition from decelerated to accelerated expansion, which is achieved by constraining a model parameter denoted as  $n$ . The deceleration parameter (DP) in Equation (29) is time-dependent, and the inflationary dynamics of the Universe are contingent upon the sign of the deceleration parameter  $q$ . A positive value of  $q$  indicates decelerating expansion, while a negative value signifies an accelerating phase in the model. With the specified parametrization of  $a(t)$ , our model alternately experiences complete acceleration and deceleration as  $t < \frac{1}{\beta} \tanh^{-1} \left(1 - \frac{1}{n}\right)^{\frac{1}{2}}$  and  $t > \frac{1}{\beta} \tanh^{-1} \left(1 - \frac{1}{n}\right)^{\frac{1}{2}}$  respectively, and it predicts transitions i.e.  $q = 0$  when  $t = \frac{1}{\beta} \tanh^{-1} \left(1 - \frac{1}{n}\right)^{\frac{1}{2}}$ . As it's widely recognized that the Universe is currently expanding at an accelerating rate, it suggests that its expansion was slower in the past [39], [40]. In these circumstances, it's sensible to use a well-thought-out approach to describe how the scale of the Universe changes over time. From Equation (29), the relation between  $\beta$  and  $n$  can be established as

$$\beta t_0 = \tanh^{-1} \left( \frac{n - q_0 - 1}{n} \right)^{\frac{1}{2}} \quad (30)$$

where  $t_0$  denotes the present time and  $q_0$  denotes the present value of DP. In this analysis, we adopt the values  $t_0 = 13.8$  and  $q_0 = -0.54$  [41] and illustrate the functions  $a(t)$ ,  $H(t)$ , and  $q(t)$  across values of  $n = 0.5, 1, 1.35$ , and  $2$ .

Using the relation

$$\frac{a}{a_0} = \frac{1}{1+z} \quad (31)$$

where  $a_0$  is present value of scale factor. Evaluating  $t(z)$ ,  $H(z)$  and  $q(z)$  in terms of redshift  $z$ , we obtain

$$t(z) = \frac{\sinh^{-1} \sqrt{\frac{n-(1+q_0)}{(z+1)^{2n}(q_0+1)}}}{\beta} \quad (32)$$

$$H(z) = \frac{\beta \coth \left( \sinh^{-1} \sqrt{\frac{n-q_0+1}{(z+1)^{2n}(q_0+1)}} \right)}{n} \quad (33)$$

$$q(z) = n - 1 - n \left[ \tanh \left( \sinh^{-1} \sqrt{\frac{n - q_0 + 1}{(z + 1)^{2n}(q_0 + 1)}} \right) \right] \quad (34)$$

In cosmology, researchers consider the EoS parameter  $\omega$  as a crucial factor explaining various cosmic regimes. More broadly,  $\omega$  can be defined as the ratio of pressure ( $p$ ) to energy density ( $\rho$ ). Specifically, when examining Equations(25) and (26), one can derive the following form;

$$\omega = \frac{(8\pi + 3\lambda)\dot{\mathcal{U}} + 3(8\pi + 2\lambda)H\mathcal{U}}{3(8\pi + 2\lambda)H\mathcal{U} - \lambda\dot{\mathcal{U}}} \quad (35)$$

Table 1: Parametric values (viz.  $\beta$ ,  $n$ ,  $q$  obtained from different datasets due to MCMC and Bayesian analysis where  $H_1 = H(z) + \text{Pantheon}$  and  $H_2 = H(z) + \text{Pantheon} + \text{BAO}$ .

Parameter	H(z)	BAO	Pantheon	$H_1$	$H_2$
$\beta$	$0.087^{+0.092}_{-0.093}$	$0.100^{+0.104}_{-0.090}$	$0.082^{+0.110}_{-0.087}$	$0.084^{+0.101}_{-0.090}$	$0.087^{+0.105}_{-0.091}$
$n$	$1.442^{+0.081}_{-0.090}$	$1.465^{+0.100}_{-0.084}$	$1.437^{+0.097}_{-0.084}$	$1.439^{+0.089}_{-0.087}$	$1.448^{+0.091}_{-0.089}$
$q$	$-0.541^{+0.010}_{-0.009}$	$-0.539^{+0.009}_{-0.011}$	$-0.540^{+0.008}_{-0.009}$	$-0.540^{+0.009}_{-0.010}$	$-0.540^{+0.009}_{-0.010}$

### 3. Observational Analysis

#### 3.1. Model parameters and observational constraints

In order to determine the relevant model parameters, we use the following datasets to draw observational constraints.

- 1. OHD:** From the cosmic chronometric approach, we have collected 55  $H(z)$  observational data points in the interval  $0 \leq z \leq 2.36$ .
- 2. BAO:** Anisotropic Baryon Acoustic Oscillation (BAO) measurements of  $D_M(z)/r_d$  and  $D_H(z)/r_d$  are included in the final BAO measurements of the SDSS collaboration. Basically this span to eight different redshift intervals (in which  $D_H(z) = c/H(z)$  is the Hubble distance and  $D_M(z)$  is the comoving angular diameter distance).
- 3. Pantheon sample:** The Pantheon sample was used to get distance modulus measurements of SN Ia [37]. The redshift range  $z \in [0.001, 2.26]$  contains 1701 light curves that correspond to 1550 distinct SN Ia events.

For the present purpose the cosmological scale factor Equation (27) led us to the Hubble Parameter Equation (33) which we use for carrying out the observational analysis. Figures 1– 6 depict 1D marginalized distribution and 2D contour diagrams for the derived model and the estimated value of the parameters extracted from OHD, BAO, Pantheon compilation of SN Ia and joined datasets respectively. The parametric values (viz.  $\beta$ ,  $n$ ,  $q$ ) obtained from different datasets due using MCMC and Bayesian analysis. The obtained values of the parameters are mentioned in the Table 1.

### 4. Energy conditions and cosmological Parameters

#### 4.1. Energy Conditions

When we consider General Relativity (GR), the Friedmann equations tell us that an accelerated expanding Universe can be achieved if  $1+3\omega < 0$ , which indicates the presence of exotic matter with negative pressure. This contradicts the usual assumption that energy density should be positive ( $\rho$ ), pointing to the possibility of nonstandard forms of matter. The different constituents that

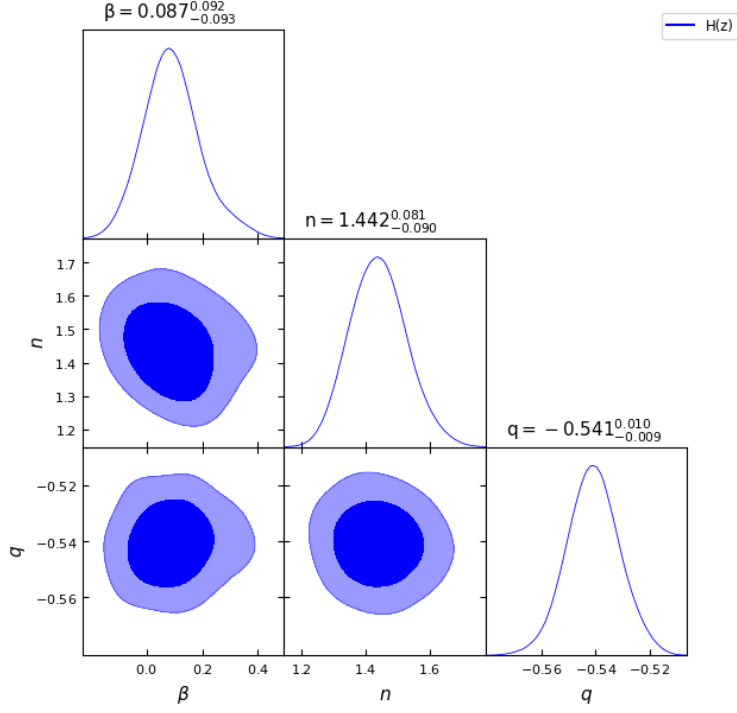


Figure 1: 1D marginalized distribution and 2D contour diagrams for the present  $f(R, T)$  model parameters with the  $H(z)$  dataset.

Table 2: Existence of various substances according to EoS parameter.

Substance	EoS parameter	Observations
Pressureless (Cold) matter	$\omega = 0$	32% of the Universe
Hot matter	$\omega \in (0, \frac{1}{3})$	Insignificant at present time
Radiation	$\omega = \frac{1}{3}$	Influential in past
Hard Universe	$\omega \in (\frac{1}{3}, 1)$	Excessive high densities
Stiff matter	$\omega = 1$	
Ekpyrotic matter	$\omega > 1$	Resist Dominant Energy Condition
Quintessence	$\omega \in (-\frac{1}{3}, -1)$	68% of the Universe
Cosmological constant	$\omega = -1$	Inconsistent with observations
Phantom Universe	$\omega < -1$	Lead to Big Rip, resist Weak Energy Condition



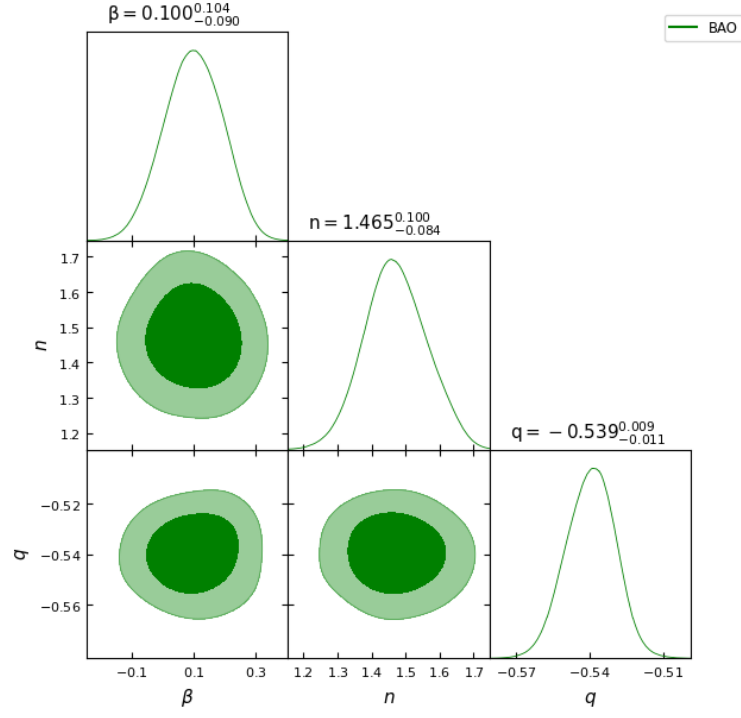


Figure 2: 1D marginalized distribution and 2D contour diagrams for the present  $f(R, T)$  model parameters with the BAO dataset.

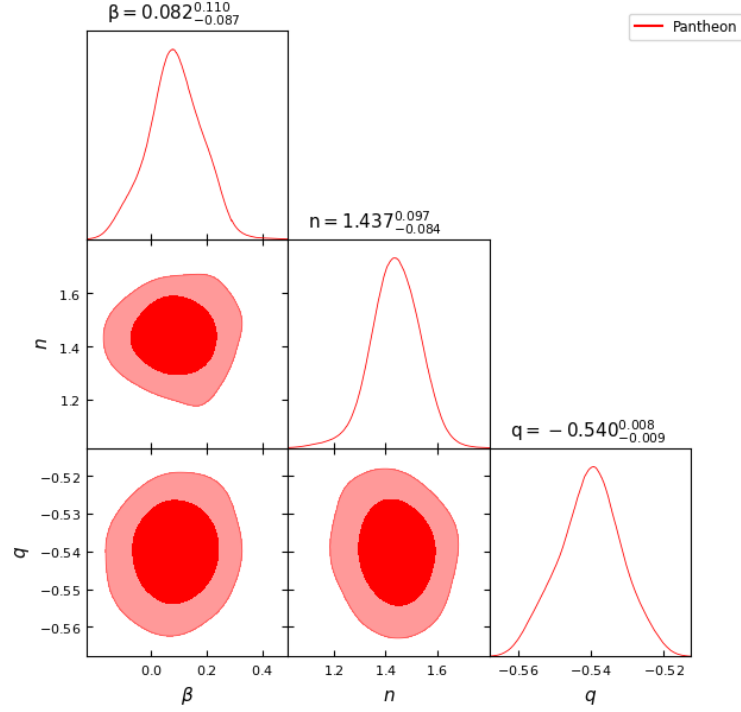


Figure 3: 1D marginalized distribution and 2D contour diagrams for the present  $f(R, T)$  model parameters with the Pantheon dataset.

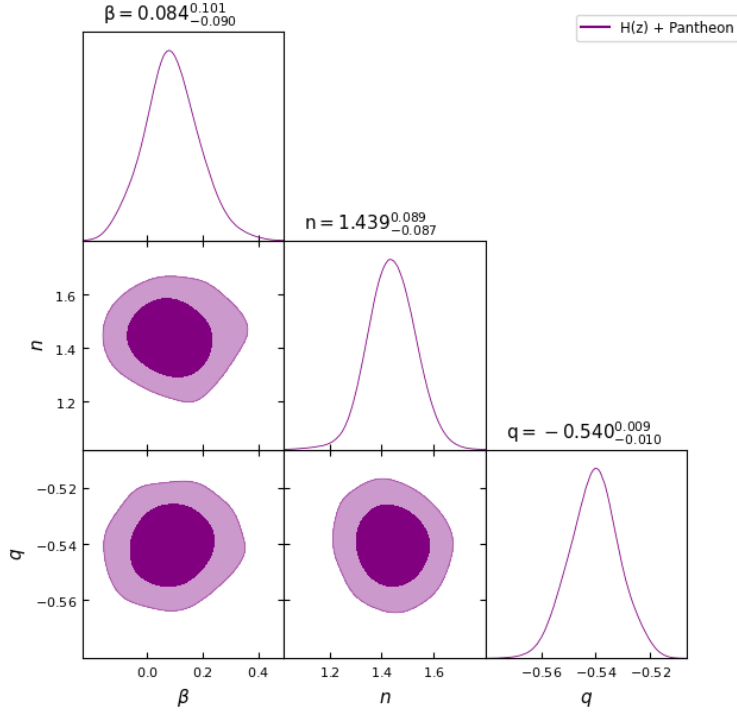


Figure 4: 1D marginalized distribution and 2D contour diagrams for the present  $f(R, T)$  model parameters with the combined  $H(z)$  and Pantheon dataset.

make up the Universe are identifiably attached to specific  $\omega$  values, and these are tabulated in Table 2.

The evolution of the Universe after its creation is conventionally divided into two epochs: radiation-dominated and matter-dominated eras. It is essential for there to exist a period when radiation dominates because, through it, one can predict whether or not primordial nucleosynthesis occurred, and any excessive deviation of more than 10% from the expansionary rate during this time would contradict data on helium abundance observed. These are both crucial periods in cosmic history: one is an era where most of the mass in the cosmos consists of elementary particles, while another is a period characterized by giant stars and supernovae explosions leading to the synthesis of heavy elements. It includes three phases – atomic, galactic, and stellar – which lasted for billions of years, ending with the present time. Each epoch plays a crucial role in forming the large-scale structures observable in the contemporary Universe.

The behavior of  $\rho$  and  $p$  from equations (25) and (26) are shown in the Figure (10) and Figure (11) highlighting the behavior of energy density  $\rho$  to be very high ( $\rho \rightarrow \infty$ ) in the beginning, and falls off as time unfolds  $\rho \rightarrow 0$  as  $t \rightarrow \infty$ .

Also, The present value of the EoS parameter for the mentioned types of evolution era can be obtained respectively, as follows:

$$\omega_0^{(n(\lambda))} = -\frac{(3\lambda + 8\pi)[3\lambda(8\alpha\beta^2 + 9) + 4\pi(8\alpha\beta^2 + 27)]}{9\lambda^2(88\alpha\beta^2 + 13) + 12\pi\lambda(320\alpha\beta^2 + 63) + 128\pi^2(35\alpha\beta^2 + 9)} \quad (36)$$

for  $n = \frac{3(\lambda+4\pi)}{2(3\lambda+8\pi)}$ , where  $\omega_0$  represents the current value of the EoS parameter. Graphically, it

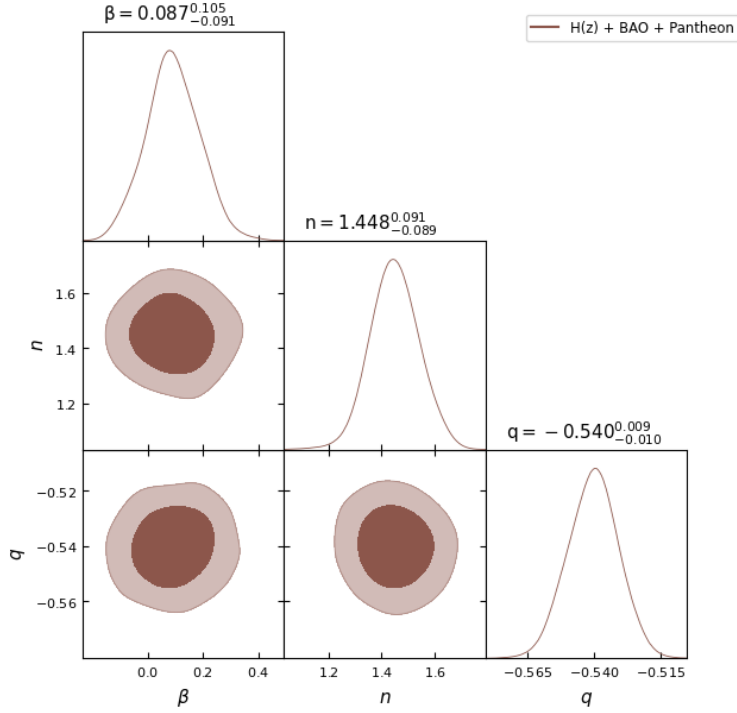


Figure 5: 1D marginalized distribution and 2D contour diagrams for the present  $f(R, T)$  model parameters with the combined  $H(z)$ , BAO and Pantheon dataset.

is represented in Figure (7) and Figure (8).

Energy conditions (EC) are instrumental in classical General Relativity (GR) because they solve the problem of spacetime singularity and explain the paths that null, space-like, time-like, or light-like geodesics follow. These have the advantage of checking for various conjectures concerning the nature of cosmological geometries and setting out what constraints should be placed on the stress-energy-momentum tensor to ensure positive energy. In general, EC can be classified as a) Null Energy Condition (NEC), b) Weak Energy Condition (WEC), c) Strong Energy Condition (SEC), and d) Dominant Energy Condition (DEC). These conditions may be stated in different forms such as geometric formulations, where EC are concisely written in terms of either Ricci tensor or Weyl tensor; physical formulations, where EC are solely outlined using the stress-energy-momentum tensor only; effective formulations, where EC are presented in terms of energy density( $\rho$ ,) which serves as time like component plus pressures( $\pi, i=1,2,3$ ), standing for spatial components. The expression for these four types of EC within GR can effectively be given point-wise as follows:

- NEC:  $\rho + p_i \geq 0, \quad \forall i,$
- WEC:  $\rho \geq 0, \rho + p_i \geq 0, \quad \forall i,$
- SEC:  $\Leftrightarrow \rho + \sum_{i=1}^3 p_i \geq 0, \quad \rho + p_i \geq 0, \quad \forall i,$
- DEC:  $\rho \geq 0, \quad p_{il} \leq p, \quad \forall i.$

The graphical representation of the Energy Conditions is shown in the Figure (9).

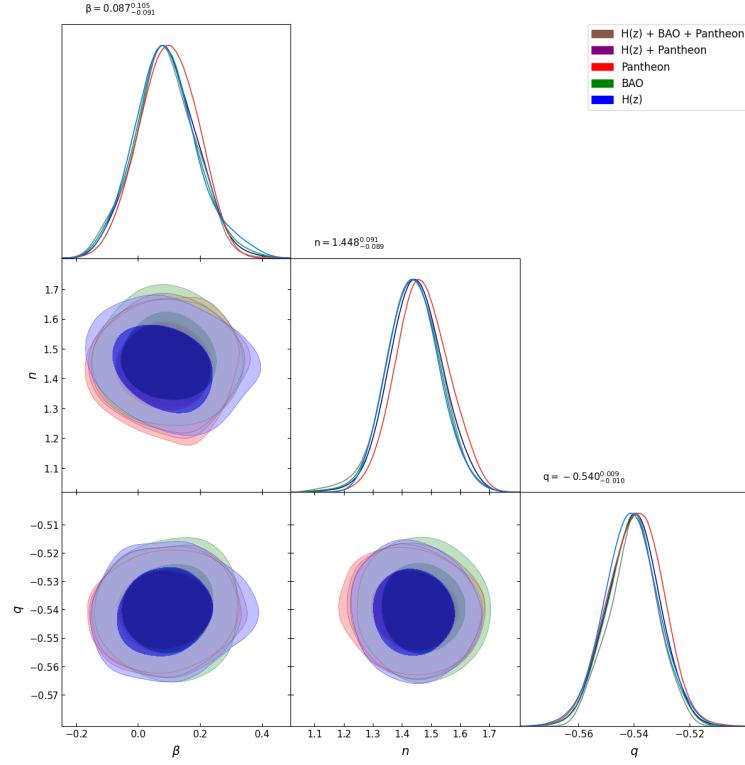


Figure 6: 1D marginalized distribution and 2D contour diagrams for the present  $f(R, T)$  model parameters with the combined variability across all datasets.

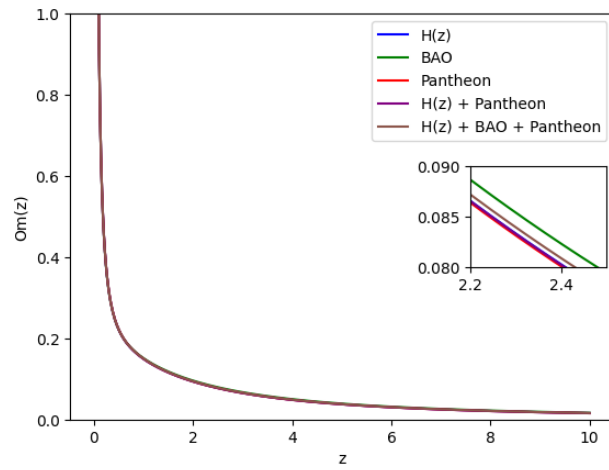


Figure 7: Plot of EoS parameter  $\omega$  vs  $z$ .

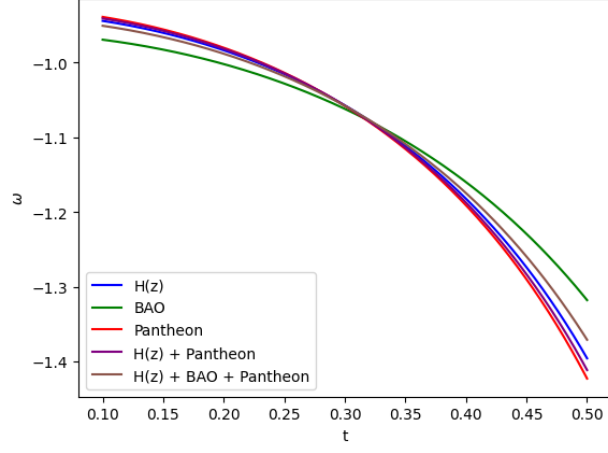


Figure 8: Plot of EoS parameter  $\omega$  vs  $t$ .

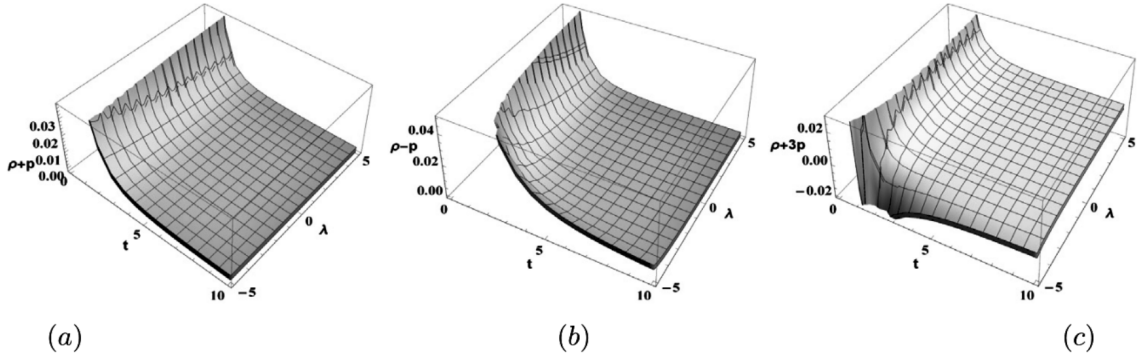


Figure 9: Graphical representation of NEC, DEC and SEC.

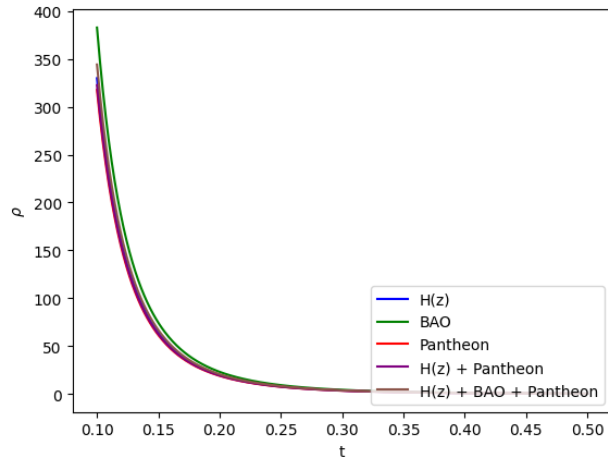


Figure 10: Illustration of the dynamic variation of the energy density over time under various parametric conditions derived from the combined  $H(z)$ , BAO and Pantheon datasets.

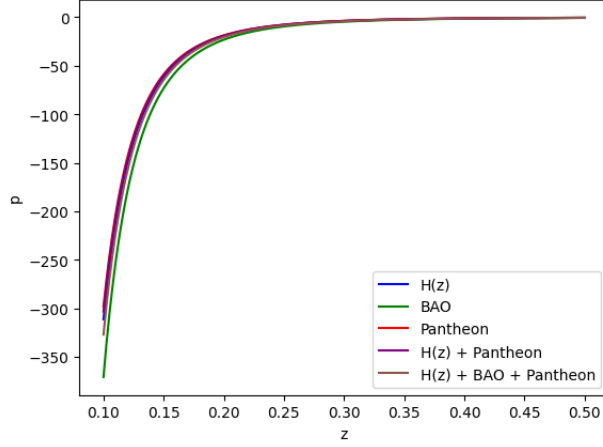


Figure 11: Using the combined  $H(z)$ , BAO, and Pantheon datasets, this figure illustrates the dynamic pressure variation over time under different parameter circumstances.

#### 4.2. State Finder Diagnostics

This universal acceleration demonstrated by new cosmological observations and the change of deceleration parameter  $q$  from positive to negative values at different redshift regions calls for a wider look beyond the  $q$  angle and Hubble parameters,  $H$ . The study aims to explore alternative models of Dark Energy (DE) to  $\Lambda$ CDM. Higher order derivatives of the scale factor  $a$ , beyond the conventional metrics of  $H$  and  $q$ , become important in understanding Universe dynamics. Consequently, we extend our analysis to include these geometric parameters concerning higher derivatives of  $a$ . For this reason, we use a diagnostic tool like the Statefinder diagnostic proposed by [42] that introduces  $r$  and  $s$  as two geometrical parameters with which DE models can be characterized. These parameters  $r$ ,  $s$  are defined as:

$$r = \frac{\ddot{a}}{aH^3}, \quad (37)$$

$$s = \frac{(-1 + r)}{3(-\frac{1}{2} + q)}. \quad (38)$$

where  $q \neq \frac{1}{2}$ . For our scale factor defined in Equation (27), the expressions of  $r$  and  $s$  can be obtained as:

$$r = 1 + n(2n - 3)\text{sech}(\beta t)^2 \quad (39)$$

$$s = \frac{4n(2n - 3)}{-9 + 12n - 9\cosh(2t\beta)} \quad (40)$$

#### 4.3. $Om(z)$ Diagnostics

The state finder parameters  $r - s$  and the  $Om(z)$  diagnostic are usually applied to analyze various dark energy ideas. Basically, the  $Om(z)$  parameter is deployed when the Hubble parameter and

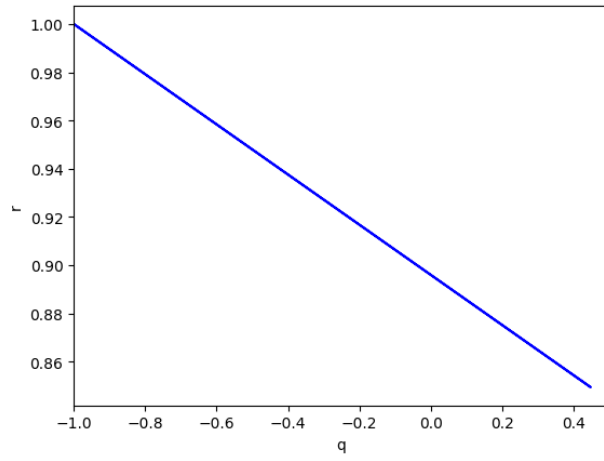


Figure 12: Graphical presentations of the state finder parameters  $r - q$ .

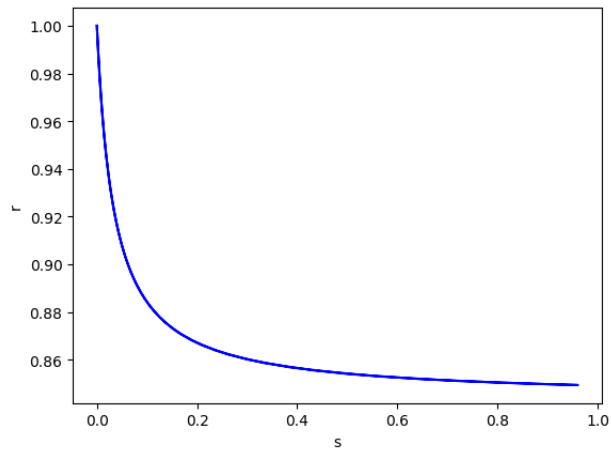


Figure 13: Graphical presentations of the state finder parameters  $r - s$ .

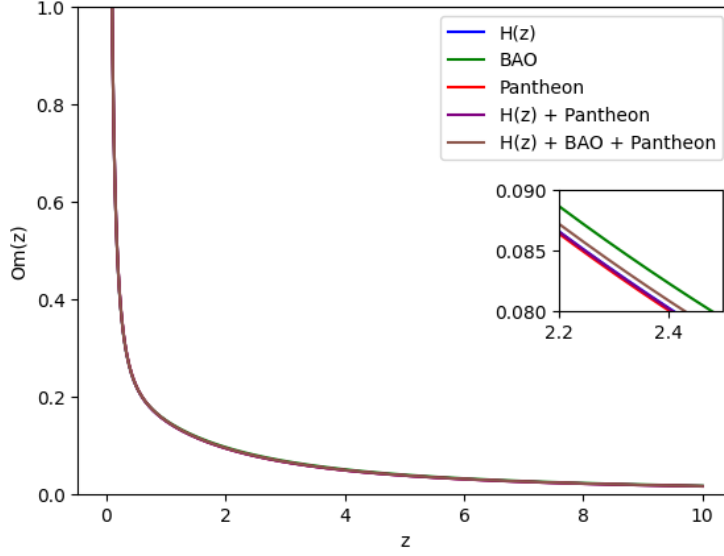


Figure 14: Graphical presentations of  $Om(z)$  with  $z$  for combined dataset based on the  $\beta$  values obtained from each dataset.

the cosmic redshift merge in a suitable way. The  $Om(z)$  parameter in the alternative gravity is read as

$$Om(z) = \frac{\left[\frac{H(z)}{H_0}\right]^2 - 1}{(1+z)^3 - 1}. \quad (41)$$

The Hubble parameter is shown by  $H_0$  in this case. Shahalam et al. [38] claim that the negative, zero and positive values of  $Om(z)$ , respectively, represent the quintessence ( $\omega \geq -1$ ),  $\Lambda$ CDM and phantom ( $\omega \leq -1$ ) dark energy theories. However, for the present model, we obtain this parameter as follows:

$$Om(z) = \frac{(1+z)^{2/b} - 1}{(1+z)^3 - 1}. \quad (42)$$

#### 4.4. Jerk Parameter

In cosmology, the Hubble parameter (H) is a crucial indicator that measures the fractional rate of change of the scale factor (a), thus describing the instantaneous expansion of the Universe. In addition to this, representing cosmic acceleration, there is a second derivative of the scale factor known as the deceleration parameter (q). A more detailed understanding and development in investigating cosmic expansion history can be achieved using higher order derivatives of scale factor, and they might help to discriminate between different dark energy models. Notably, this quantity measures how fast the third derivative of the scale factor concerning time changes (t). Expanding the Taylor series for scale factor about some reference value ( $a_0$ ), considering the fourth term reveals the jerk parameter = j. The Taylor expansion, centers around the value  $a_0$  is,

$$\frac{a}{a_0} = 1 + H_0 t - \frac{1}{2!} q_0 H_0^2 t^2 + \frac{1}{3!} j_0 H_0^3 t^3 - \dots, \quad (43)$$



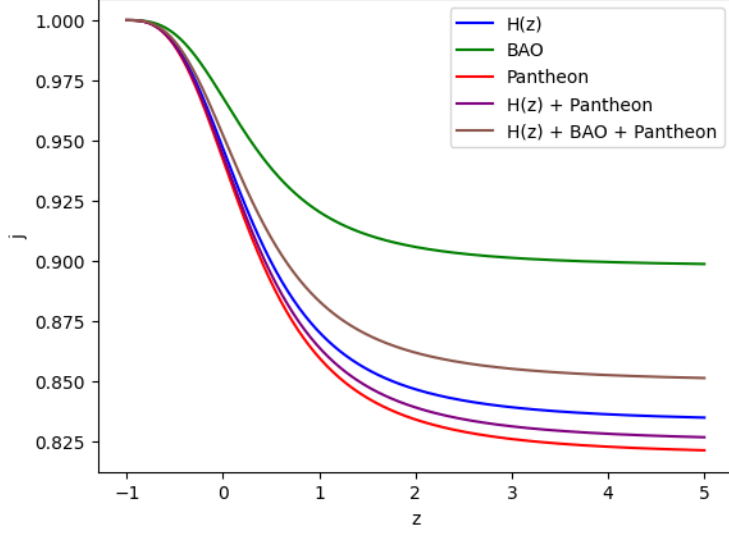


Figure 15: Graphical presentation of the jerk parameter vs redshift.

where  $H_0$ ,  $q_0$  and  $j_0$  being the current values of the parameters. Thus, we can define the jerk parameter as;

$$j = \frac{\ddot{a}}{aH^3}, \quad (44)$$

and in terms of  $q$ , jerk parameter can be defined as;

$$j = q + 2q^2 - \frac{\dot{q}}{H} \quad (45)$$

Substituting Equation (27) and Equation (28), we get

$$j = 1 + n(2n - 3)\text{sech}(\beta t)^2. \quad (46)$$

Also, we can represent jerk parameter  $j$  in terms of redshift  $z$  for given  $q(z)$  and it takes the form;

$$j = 1 + \frac{n(2n - 3)}{1 + 2.17391(n - 0.46)(1 + z)^{-2n}} \quad (47)$$

As shown in Figure (15), this is how we can describe how the Universe behaves dynamically within the cosmic jerk. The change from a decelerating phase to an accelerating one is characterized by  $j$  (the cosmic jerk parameter) being positive at about  $j_0 \approx 1$  and  $q_0$ , the deceleration parameter, having a negative value as predicted by the  $\Lambda$ CDM model. The behavior of  $j$  over various values of  $n$  obtained using the data sets  $H(z)$ , BAO, Pantheon and their combinations demonstrates that it continues to be positive for all cases while tending towards unity for later ages. Remarkably, although the present-day jerk parameter (at  $z = 0$ ) is still larger than 1, it differs from unity in all cases considered here. Thus, these results imply the possibility of some other dark energy model that is not based on the  $\Lambda$ CDM paradigm.

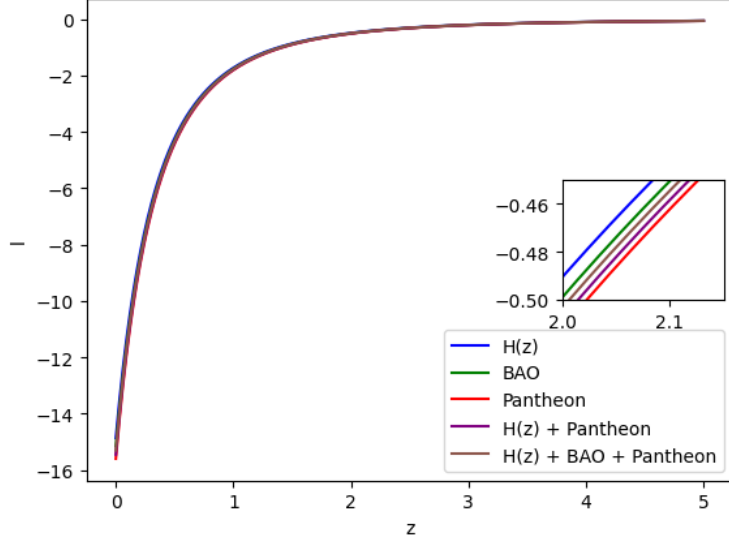


Figure 16: Graphical presentation of the lerk parameter vs redshift.

#### 4.5. Lerk and Snap Parameter

Many cosmological parameters, given as higher-order derivatives of the scalar component, are examined to comprehend the universe's expansion history better. As a result, these characteristics are extremely useful for investigating the dynamics of the cosmos. For example, the Hubble parameter  $H$  depicts the universe's expansion rate, the deceleration parameter  $q$  depicts the universe's phase transition, and the jerk parameter  $j$ , snap parameter  $s$ , and lerk parameter  $l$  study dark energy theories and their dynamics. These are as follows:

$$H = \frac{\dot{a}}{a} \quad (48)$$

$$q = \frac{\ddot{a}}{aH^2} \quad (49)$$

$$j = \frac{\dddot{a}}{aH^3} \quad (50)$$

$$s = \frac{\ddddot{a}}{aH^4} \quad (51)$$

$$l = \frac{\dddot{\ddot{a}}}{aH^5} \quad (52)$$

Lerk and Snap parameters are graphically shown in Figure (16) and Figure (17), respectively, for different values of  $n$  obtained using a combination of datasets.

## 5. Conclusion

In the present work our aim was to find the possibility of a Hyperbolic Cosmological model under the background of FLRW metric of  $f(R, T)$  gravity with the form  $f(R, T) = f(R) + 2f(T)$ .

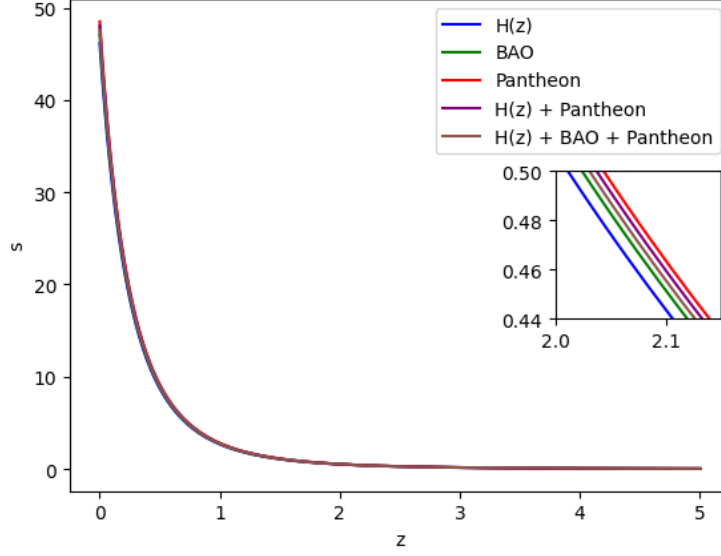


Figure 17: Graphical presentation of the snap parameter vs redshift.

In recent cosmological analysis, the usefulness of  $f(R)$  as a functional expression is questioned to add quadratic geometric corrections in General Relativity (GR) models in line with experimental results. Considering variable  $T$  as a trace of EMT makes incorporating exotic imperfect fluids and quantum effects possible. Additionally, the non-minimal matter-geometry coupling concept may be understood from the functional form of  $T$  as per previous studies. This enables all field equations that define the evolution of the Universe to be precisely formulated within a general action for  $f(R, T)$ . Therefore, interpreting these equations becomes very significant through extensive statistical analyses and observational data for understanding complicated dynamics inherent in cosmology.

The investigation provides the following salient features:

- i. To compare the model parameters with the observational data, we impose constraints on the model using the datasets from the Hubble parameter  $H(z)$ , BAO, Pantheon, combined  $H(z) + \text{Pantheon}$ , and combined  $H(z) + \text{BAO} + \text{Pantheon}$ . The outcomes for  $\beta$ ,  $n$  and  $q$  under our  $f(R, T)$  gravity model are as follows:  $\beta = 0.087^{+0.092}_{-0.093}$ ,  $\beta = 0.100^{+0.104}_{-0.090}$ ,  $\beta = 0.082^{+0.110}_{-0.087}$ ,  $\beta = 0.084^{+0.101}_{-0.090}$ ,  $\beta = 0.087^{+0.105}_{-0.091}$ ,  $n = 1.442^{+0.081}_{-0.090}$ ,  $n = 1.465^{+0.100}_{-0.084}$ ,  $n = 1.437^{+0.097}_{-0.084}$ ,  $n = 1.439^{+0.089}_{-0.087}$ ,  $n = 1.448^{+0.091}_{-0.089}$ ,  $q = -0.541^{+0.010}_{-0.009}$ ,  $q = -0.539^{+0.009}_{-0.011}$ ,  $q = -0.540^{+0.008}_{-0.009}$ ,  $q = -0.540^{+0.009}_{-0.010}$ ,  $q = -0.540^{+0.009}_{-0.010}$ , respectively.
- ii. We have addressed the energy conditions,  $Om(z)$  analysis, and cosmographical parameters, which are equivocally very responsive and informative for the physical viability of our model.
- iii. Graphical presentations of different model parameters are shown in several figures, which are very informative in their nature. Considering the relationship between the state parameter of the equation and the passage of time, implies that dark energy plays a role in the accelerated expansion of the universe, while its exact nature varies over time. This finding could have

intriguing cosmological implications.

Overall observation and conclusion can be put forward as follows: the obtained results demonstrate that the proposed model mostly agrees with the observational signatures of the cosmological scenario within a certain range of restrictions.

## Data Availability

This research did not yield any new data..

## Conflict of Interest

The authors declare no conflict of interest.

## Acknowledgement

SR would like to express his gratitude to the ICARD facilities at CCASS, GLA University, Mathura, as well as the Visiting Research Associateship Programme at the Inter-University Centre for Astronomy and Astrophysics (IUCAA) in Pune, India.

## References

- [1] Chanchal Chawla, R. K. Mishra, and Anirudh Pradhan, *Anisotropic Bianchi-I Cosmological Models in String Cosmology with Variable Deceleration Parameter*, *arXiv:1203.4014* [physics.gen-ph] (2012).
- [2] Tiberiu Harko, Francisco S. N. Lobo, Shin'ichi Nojiri, and Sergei D. Odintsov,  *$f(R, T)$  gravity*, *Physical Review D*, **84**(2), 024020 (2011). <http://dx.doi.org/10.1103/PhysRevD.84.024020>.
- [3] A. A. Starobinsky, *Phys. Lett. B* **91** (1980), 99-102 doi:10.1016/0370-2693(80)90670-X
- [4] Planck Collaboration, P. A. R. Ade, N. Aghanim, M. Arnaud, M. Ashdown, J. Aumont, C. Baccigalupi, A. J. Banday, R. B. Barreiro, J. G. Bartlett, N. Bartolo, E. Battaner, R. Battye, K. Benabed, A. Benoît, A. Benoit-Lévy, J. -P. Bernard, M. Bersanelli, P. Bielewicz, J. J. Bock, A. Bonaldi, L. Bonavera, J. R. Bond, J. Borrill, F. R. Bouchet, F. Boulanger, M. Bucher, C. Burigana, R. C. Butler, E. Calabrese, J. -F. Cardoso, A. Catalano, A. Challinor, A. Chamballu, R. -R. Chary, H. C. Chiang, J. Chluba, P. R. Christensen, S. Church, D. L. Clements, S. Colombi, L. P. L. Colombo, C. Combet, A. Coulais, B. P. Crill, A. Curto, F. Cuttaia, L. Danese, R. D. Davies, R. J. Davis, P. de Bernardis, A. de Rosa, G. de Zotti, J. Delabrouille, F. -X. Désert, E. Di Valentino, C. Dickinson, J. M. Diego, K. Dolag, H. Dole, S. Donzelli, O. Doré, M. Douspis, A. Ducout, J. Dunkley, X. Dupac, G. Efstathiou, F. Elsner, T. A. Enßlin, H. K. Eriksen, M. Farhang, J. Fergusson, F. Finelli, O. Forni, M. Frailis, A. A. Fraisse, E. Franceschi, A. Frejsel, S. Galeotta, S. Galli, K. Ganga, C. Gauthier, M. Gerbino, T. Ghosh, M. Giard, Y. Giraud-Héraud, E. Giusarma, E. Gjerløw, J. González-Nuevo, K. M. Górski, S. Gratton, A. Gregorio, A. Gruppuso, J. E. Gudmundsson, J. Hamann, F. K. Hansen, D. Hanson, D. L. Harrison, G. Helou, S. Henrot-Versillé, C. Hernández-Monteagudo, D. Herranz, S. R. Hildebrandt, E. Hivon, M. Hobson, W. A. Holmes, A. Hornstrup, W. Hovest, Z. Huang, K. M. Huffenberger, G. Hurier, A. H. Jaffe, T. R. Jaffe, W. C. Jones, M. Juvela, E. Keihänen, R. Keskitalo, T. S. Kisner, R. Kneissl, J. Knoche, L. Knox, M. Kunz, H. Kurki-Suonio, G. Lagache, A. Lähteenmäki, J. -M. Lamarre, A. Lasenby, M. Lattanzi, C. R. Lawrence, J. P. Leahy, R. Leonardi, J. Lesgourgues, F. Levrier, A. Lewis, M. Liguori, P. B. Lilje, M. Linden-Vørnle, M. López-Caniego, P. Lubin, J. F. Macías-Pérez, G. Maggio, D. Maino, N. Mandolesi, A. Mangilli, A. Marchini, M. Maris, P. G. Martin, M. Martinelli, E. Martínez-González, S. Masi, S. Matarrese, P. McGehee, P. R. Meinhold, A. Melchiorri, J. -B. Melin, L. Mendes, A. Mennella, M. Migliaccio, M. Millea, S. Mitra, M. -A. Miville-Deschênes, A. Moneti, L. Montier, G. Morgante, D. Mortlock, A. Moss, D. Munshi, J. A. Murphy, P. Naselsky, F. Nati, P. Natoli, C. B. Netterfield, H. U. Nørgaard-Nielsen, F. Noviello, D. Novikov,

- I. Novikov, C. A. Oxborrow, F. Paci, L. Pagano, F. Pajot, R. Paladini, D. Paoletti, B. Partridge, F. Pasian, G. Patanchon, T. J. Pearson, O. Perdureau, L. Perotto, F. Perrotta, V. Pettorino, F. Piacentini, M. Piat, E. Pierpaoli, D. Pietrobon, S. Plaszczynski, E. Pointecouteau, G. Polenta, L. Popa, G. W. Pratt, G. Pr  zeau, S. Prunet, J. -L. Puget, J. P. Rachen, W. T. Reach, R. Rebolo, M. Reinecke, M. Remazeilles, C. Renault, A. Renzi, I. Ristorcelli, G. Rocha, C. Rosset, M. Rossetti, G. Roudier, B. Rouill   d'Orfeuil, M. Rowan-Robinson, J. A. Rubi  no-Mart  n, B. Rusholme, N. Said, V. Salvatelli, L. Salvati, M. Sandri, D. Santos, M. Savelainen, G. Savini, D. Scott, M. D. Seiffert, P. Serra, E. P. S. Shellard,
- [5] J. D. Barrow and S. Cotsakis, *Phys. Lett. B* **214** (1988), 515-518 doi:10.1016/0370-2693(88)90110-4
  - [6] B. C. Paul, P. S. Debnath, and S. Ghose, *Accelerating universe in modified theories of gravity*, *Physical Review D*, **79**(8), 083534 (2009). <http://dx.doi.org/10.1103/PhysRevD.79.083534>.
  - [7] B. Wang, E. Abdalla, F. Atrio-Barandela and D. Pavon, Dark Matter and Dark Energy Interactions: Theoretical Challenges, Cosmological Implications and Observational Signatures, *Rept. Prog. Phys.* **79**, 096901 (2016)
  - [8] P. J. E. Peebles and B. Ratra, The Cosmological Constant and Dark Energy, *Rev. Mod. Phys.* **75**, 559-606 (2003)
  - [9] T. Padmanabhan, Cosmological constant: The Weight of the vacuum, *Phys. Rept.* **380**, 235-320 (2003)
  - [10] E. Abdalla and A. Marins, The Dark Sector Cosmology, *Int. J. Mod. Phys. D* **29**, 2030014 (2020)
  - [11] M. Li, X. D. Li, S. Wang and Y. Wang, Dark Energy: A Brief Review, *Front. Phys. (Beijing)* **8**, 828-846 (2013)
  - [12] V. Sahni, The Cosmological constant problem and quintessence, *Class. Quant. Grav.* **19**, 3435-3448 (2002)
  - [13] J. Garriga and A. Vilenkin, Solutions to the cosmological constant problems, *Phys. Rev. D* **64**, 023517 (2001)
  - [14] J. Frieman, M. Turner and D. Huterer, Dark Energy and the Accelerating Universe, *Ann. Rev. Astron. Astrophys.* **46**, 385-432 (2008)
  - [15] S. Nojiri and S. D. Odintsov, Unified cosmic history in modified gravity: from  $F(R)$  theory to Lorentz non-invariant models, *Phys. Rept.* **505**, 59-144 (2011)
  - [16] L. Samushia and B. Ratra, Constraining dark energy with gamma-ray bursts, *Astrophys. J.* **714**, 1347-1354 (2010)
  - [17] M. Yashar, B. Bozek, A. Abrahamse, A. Albrecht and M. Barnard, Exploring Parameter Constraints on Quintessential Dark Energy: the Inverse Power Law Model, *Phys. Rev. D* **79**, 103004 (2009)
  - [18] Harko, Tiberiu, Francisco SN Lobo, Shin'ichi Nojiri, and Sergei D. Odintsov,  $f(R, T)$  gravity, *Phys. Rev. D* **84**, 024020 (2011)
  - [19] T. Harko, Thermodynamic interpretation of the generalized gravity models with geometry - matter coupling, *Phys. Rev. D* **90**, no.4, 044067 (2014)
  - [20] L. K. Sharma, A. K. Yadav, P. K. Sahoo and B. K. Singh, Non-minimal matter-geometry coupling in Bianchi I space-time, *Res. Phys.* **10**, 738-742 (2018)
  - [21] A. K. Yadav, L. K. Sharma, B. K. Singh and P. K. Sahoo, Existence of bulk viscous universe in  $f(R, T)$  gravity and confrontation with observational data, *New Astron.* **78**, 101382 (2020)
  - [22] L. K. Sharma, A. K. Yadav and B. K. Singh, Power-law solution for homogeneous and isotropic universe in  $f(R, T)$  gravity, *New Astron.* **79**, 101396 (2020)
  - [23] L. K. Sharma, B. K. Singh and A. K. Yadav, Viability of Bianchi type V universe in  $f(R, T) = f_1(R) + f_2(R)f_3(T)$  gravity, *Int. J. Geom. Meth. Mod. Phys.* **17**, 2050111 (2020)
  - [24] S. Nojiri and S. D. Odintsov, Unified cosmic history in modified gravity: from  $F(R)$  theory to Lorentz non-invariant models, *Phys. Rept.* **505**, 59-144 (2011)
  - [25] S. M. Carroll, V. Duvvuri, M. Trodden and M. S. Turner, Is cosmic speed-up due to new gravitational physics? *Phys. Rev. D* **70**, 043528 (2004)
  - [26] W. Hu and I. Sawicki, Models of  $f(R)$  Cosmic Acceleration that Evade Solar-System Tests, *Phys. Rev. D* **76**, 064004 (2007)
  - [27] F. G. Alvarenga, A. de la Cruz-Dombriz, M. J. S. Houndjo, M. E. Rodrigues and D. S  ez-G  mez, Dynamics of scalar perturbations in  $f(R, T)$  gravity, *Phys. Rev. D* **87**, 103526 (2013)
  - [28] P. K. Sahoo, P. Sahoo and B. K. Bishi, Anisotropic cosmological models in  $f(R, T)$  gravity with variable deceleration parameter, *Int. J. Geom. Meth. Mod. Phys.* **14**, 1750097 (2017)
  - [29] Z. Yousaf, K. Bamba and M. Z. u. H. Bhatti, Causes of Irregular Energy Density in  $f(R, T)$  Gravity, *Phys. Rev. D* **93**, 124048 (2016)
  - [30] Z. Yousaf, M. Z. u. H. Bhatti and M. Ilyas, Existence of compact structures in  $f(R, T)$  gravity, *Eur. Phys. J. C* **78**, 307 (2018)
  - [31] Z. Yousaf, K. Bamba and M. Z. u. H. Bhatti, Influence of Modification of Gravity on the Dynamics of Radiating Spherical Fluids, *Phys. Rev. D* **93**, 064059 (2016)

- [32] Z. Yousaf, K. Bamba, M. Z. Bhatti and U. Ghafoor, Charged Gravastars in Modified Gravity, *Phys. Rev. D* **100**, 024062 (2019)
- [33] A. Das, F. Rahaman, B. K. Guha and S. Ray, Compact stars in  $f(R, T)$  gravity, *Eur. Phys. J. C* **76**, 654 (2016)
- [34] A. K. Yadav, P. K. Sahoo and V. Bhardwaj, Bulk viscous Bianchi-I embedded cosmological model in  $f(R, T) = f_1(R) + f_2(R)f_3(T)$  gravity, *Mod. Phys. Lett. A* **34**, 1950145 (2019)
- [35] S. V. Lohakare, B. Mishra, S. K. Maurya, Ksh. N. Singh, Analyzing the Geometrical and Dynamical Parameters of Modified Teleparallel- Gauss-Bonnet Model, arXiv: 2209.13197.
- [36] S. Alam et al. (eBOSS), Completed SDSS-IV extended Baryon Oscillation Spectroscopic Survey: Cosmological implications from two decades of spectroscopic surveys at the Apache Point Observatory, *Phys. Rev. D* **103**, 083533 (2021).
- [37] D. M. Scolnic et al., The Complete Light-curve Sample of Spectroscopically Confirmed SNe Ia from Pan-STARRS1 and Cosmological Constraints from the Combined Pantheon Sample, *Astrophys. J.* 859, 101 (2018).
- [38] M. Shahalam, S. Sami and A. Agarwa, *Mon. Not. R. Astron. Soc.* **448**, 2948 (2015).
- [39] A. G. Riess, A. V. Filippenko, P. Challis, A. Clocchiatti, A. Diercks, P. M. Garnavich, R. L. Gilliland, C. J. Hogan, S. Jha, R. P. Kirshner, B. Leibundgut, M. M. Phillips, D. Reiss, B. P. Schmidt, R. A. Schommer, R. C. Smith, J. Spyromilio, C. Stubbs, N. B. Suntzeff, and J. Tonry, "Observational Evidence from Supernovae for an Accelerating Universe and a Cosmological Constant," *The Astronomical Journal*, vol. 116, no. 3, pp. 1009–1038, American Astronomical Society, Sep. 1998, <http://dx.doi.org/10.1086/300499>.
- [40] S. Perlmutter, G. Aldering, G. Goldhaber, R. A. Knop, P. Nugent, P. G. Castro, S. Deustua, S. Fabbro, A. Goobar, D. E. Groom, I. M. Hook, A. G. Kim, M. Y. Kim, J. C. Lee, N. J. Nunes, R. Pain, C. R. Pennypacker, R. Quimby, C. Lidman, R. S. Ellis, M. Irwin, R. G. McMahon, P. Ruiz-Lapuente, N. Walton, B. Schaefer, B. J. Boyle, A. V. Filippenko, T. Matheson, A. S. Fruchter, N. Panagia, H. J. M. Newberg, W. J. Couch, The Supernova Cosmology Project, "Measurements of  $\Omega$  and  $\Lambda$  from 42 High-Redshift Supernovae," *The Astrophysical Journal*, vol. 517, no. 2, pp. 565–586, Jun. 1999, <https://ui.adsabs.harvard.edu/abs/1999ApJ...517..565P>, doi:10.1086/307221.
- [41] A. A. Mamon and S. Das, "A parametric reconstruction of the deceleration parameter," *The European Physical Journal C*, vol. 77, no. 7, Jul. 2017, <http://dx.doi.org/10.1140/epjc/s10052-017-5066-4>, doi:10.1140/epjc/s10052-017-5066-4.
- [42] V. Sahni, T. D. Saini, A. A. Starobinsky, and U. Alam, "Statefinder—A new geometrical diagnostic of dark energy," *Journal of Experimental and Theoretical Physics Letters*, vol. 77, no. 5, pp. 201–206, Mar. 2003, <http://dx.doi.org/10.1134/1.1574831>, doi:10.1134/1.1574831.